



Wavelet-based multi-scale projection method in homogenization of heterogeneous media

Shafigh Mehraeen, Jiun-Shyan Chen*

*Department of Civil and Environmental Engineering, University of California, Los Angeles,
5731G Boelter Hall, Los Angeles, CA 90095-1593, USA*

Received 15 December 2003; accepted 11 January 2004

Abstract

Standard homogenization of highly heterogeneous media often filters out the fine scale information, and as a consequence, it produces acceptable results only for certain type of periodic structures. In this work, a wavelet-based multi-scale homogenization is introduced for highly heterogeneous materials where the standard asymptotic technique cannot be effectively applied. A set of scaling and wavelet functions based on the linear hat function and its corresponding wavelet transformation matrix are constructed. The advantages of this wavelet transformation constructed by hat function compared to that formulated using Haar function are identified. The mirror image technique has been employed to preserve the accurate representation of boundary conditions and to avoid numerical oscillation near the boundaries. This wavelet-based multi-scale transformation hierarchically filters out the high-scale components of the solution, and thus provides an effective framework for the multi-scale selection of the most essential scales of the solution.

© 2004 Elsevier B.V. All rights reserved.

Keywords: Wavelet; Multi-scale homogenization; Heterogeneous media

1. Introduction

The objective of homogenization is to construct simpler fine scale equations which are considerably less expensive to solve and whose solutions have the same coarse scale properties as the solutions of the complicated systems. The classical theory of homogenization developed by Bensoussan et al. [1] considers the following boundary value problem:

$$L_\epsilon u_\epsilon = f \quad \text{in } \Omega \tag{1}$$

* Corresponding author.

E-mail address: jschen@seas.ucla.edu (J.-S. Chen).

subjected to appropriate boundary conditions which is well posed in Sobolov space H for all ε . Here ε is a small parameter such that $u_\varepsilon \rightarrow \bar{u}$ as $\varepsilon \rightarrow 0$, where \bar{u} is the homogenized solution. The problem of homogenization is to find the differential equation that \bar{u} satisfies and to construct the corresponding differential operator. Several methods have been proposed for solving homogenization problems.

The first method is homogenized Dirichlet projection method which was developed based on the concept of hierarchical modeling. In this method, the mathematical model at the coarsest level is represented by homogenized material properties. This is referred to as the homogenized problem, and the exclusion of heterogeneity generally makes the homogenized problem computationally inexpensive compared to models of finer scale. Using a posteriori modeling error, the accuracy of the solution capable of representing the homogenized behavior of the original heterogeneous problem is estimated. In regions where the modeling error exceeds a preset tolerance, a finer scale model is used and a correction to the homogenized solution is made. This homogenization procedure is continued until the error tolerance is met [2].

In the method of asymptotic expansion [1], the relationship between the macroscopic and microscopic solution can be derived, and the corresponding homogenized differential operator and homogenized coefficients for solving the macroscopic solution can be obtained. The microscopic solution is obtained by solving a unit cell problem with periodic boundary conditions. Alternatively, a multi-grid method for a periodic heterogeneous medium has been introduced [3]. In this approach, a multi-grid method is employed to develop a fast iterative solver for differential equations with oscillatory coefficients as in Eq. (1). An intergrid transfer operator is constructed following the asymptotic expansion so that the problem on the auxiliary grid gives rise to a homogenization problem. The basic limitation of these two methods is that they necessitate the fine scale response of the material to be fairly separated from the response on the coarser scales.

In the recent multiresolution approach given in [4,5], an equation for the coarse scale component of the solution can be directly constructed. Utilizing the notion of the multiresolution analysis (MRA), the transformation between two different scales is explicitly defined. This process is based on the reduction (static condensation) which involves computing the Schur complement of fine scale. The reduction procedure can be repeated over several scales, therefore it does not require the small parameter assumption ($\varepsilon \rightarrow 0$ in Eq. (1)) which is typical for asymptotic methods [6]. Knappek [7] has applied Schur complement for a multi-grid-based homogenization technique. Moreover, multiresolution strategy using wavelet functions for reduction and homogenization has been applied to system of linear ordinary differential equations [4]. Specific form of these wavelets known as Haar basis has also been applied in the framework of Galerkin method (wavelet Galerkin method) [8]. It has been demonstrated that wavelet Galerkin method creates a hierarchical representation of the homogenized solution at different scales and subsequently the multiresolution properties of the wavelet functions are exploited to smoothen the inhomogeneity in the multi-scale solution of the differential equation.

In this paper, we propose the wavelet-based projection method by means of introducing wavelet functions as bases for multi-scale homogenization of an elasticity problem with oscillatory coefficients. The content of this paper is organized as follows. The fundamental equations of wavelet functions and transformation are discussed in Section 2. The wavelet-based homogenization technique for decomposition of the coarse and fine scale solutions is presented in Section 3. In Section 4, data compactness and mirror image technique are discussed. We analyze three numerical examples to demonstrate the effectiveness of the proposed method in Section 5 followed by concluding remarks in Section 6.

2. Wavelet spaces

In this section, the process of filtering a function into low and high scale contents based on the wavelet theory [9–11] is shown. In this discussion, we first define two intimately related functions, namely the scaling function $\varphi(x)$ and its corresponding wavelet function $\psi(x)$. A multiresolution analysis is defined by a nested sequence of closed subspace $\{V_j\}_{j \in \mathbb{Z}}$ with the properties as follows:

$$\cdots \subset V_{-1} \subset V_0 \subset V_1 \subset \cdots \subset L^2(R), \tag{2}$$

$$\overline{\bigcup_{j \in \mathbb{Z}} V_{-j}} = L^2(R), \tag{3}$$

$$\bigcap_{j \in \mathbb{Z}} V_j = \{0\}. \tag{4}$$

Each subspace V_j of scale j is spanned by a set of scaling functions $\{\varphi_{j,k}(x), \forall k \in \mathbb{Z}\}$:

$$V_j = \{\varphi_{j,k}(x) | \varphi_{j,k}(x) = 2^{\frac{j}{2}} \varphi(2^j x - k)\}. \tag{5}$$

The relation between coarse and fine scaling functions can be defined through the dilation and translation laws in Eqs. (6) and (7), respectively,

$$\varphi(x) \in V_j \Leftrightarrow \varphi(2x) \in V_{j+1}, \quad j \in \mathbb{Z}, \tag{6}$$

$$\varphi(x) \in V_0 \Leftrightarrow \varphi(x - n) \in V_0, \quad \text{for all } n \in \mathbb{Z}. \tag{7}$$

A mutually orthogonal complement of V_j in V_{j+1} is denoted by a subspace W_j associated with the multiresolution analysis such that

$$V_{j+1} = V_j \oplus W_j, \quad \forall j \in \mathbb{Z}, \tag{8}$$

where \oplus is a direct sum. Similar to V_j , W_j is formed by another orthogonal basis

$$\psi_{j,k}(x) = 2^{\frac{j}{2}} \psi(2^j x - k), \tag{9}$$

where $\psi(x)$ is the mother wavelet.

The wavelet $\psi(x)$ is chosen to be a function orthogonal to the scaling function with respect to translation. Using Eqs. (2) and (8), one has

$$\bigoplus_{j \in \mathbb{Z}} W_j = L^2(R). \tag{10}$$

Based on the definition in Eq. (8), it follows that

$$V_j = V_i \oplus \left(\bigoplus_{k=0}^{j-i-1} W_{i+k} \right), \quad j > i. \tag{11}$$

The functions $\varphi_{j,k}$ in Eq. (5) generate an L_2 -orthogonal basis. These functions are orthogonal under translation. We note that for a fixed j , $\varphi_{j,k}$ span the whole function space and we can approximate any function using $\varphi_{j,k}$ as a basis:

$$P_j f = \sum_{k=-\infty}^{\infty} c_k \varphi_{j,k}, \tag{12}$$

where P_j is the operator projecting f onto the subspace V_j spanned by $\varphi_{j,k}$. One can change the scale of the function by changing j to improve the accuracy of the approximation. The two-scale relation for the scaling functions can be written as

$$\varphi(x) = \sqrt{2} \sum_{n=-\infty}^{\infty} d_n \varphi(2x - n). \tag{13}$$

By imposing the orthogonality conditions between scaling and wavelet functions in the frequency domain using Fourier transform, an orthogonal wavelet function can be expressed as

$$\psi(x) = \sqrt{2} \sum_{n=-\infty}^{\infty} (-1)^{n-1} d_{-n-1} \varphi(2x - n), \tag{14}$$

where d_n is the wavelet coefficient calculated by applying the orthogonality conditions to scaling functions with respect to translation parameter. Orthogonal scaling function can be constructed by choosing a candidate function $\varphi^*(x)$ such that $\varphi^*(x)$ and its Fourier transform have a reasonable decay and a finite support. In addition,

$$\int \varphi^*(x) dx \neq 0. \tag{15}$$

Moreover, the candidate function should satisfy the two-scale relation

$$\varphi^*(x) = \sum_n c_n \varphi^*(2x - n), \quad n \in \mathbb{Z}. \tag{16}$$

With a selected candidate function, the orthogonal scaling function $\varphi(x)$ is expressed in terms of $\varphi^*(x)$ by

$$\varphi(x) = \sum_{n=-\infty}^{\infty} a_n \varphi^*(x - n). \tag{17}$$

Note that Eqs. (13) and (14) are the algorithm for construction of scaling and wavelet functions of coarser scale in term of scaling function of finer scale. Conversely, using these two equations, one can also derive the decomposition relation as

$$\varphi(2x - l) = \sum_{k=-\infty}^{\infty} d_{l-2k} \varphi(x - k) + \sum_{k=-\infty}^{\infty} b_{l-2k} \psi(x - k), \quad l \in \mathbb{Z}, \tag{18}$$

which illustrates the decomposition of scaling function of the finer scale in terms of scaling and wavelet functions of the coarser scale. In case of Haar system, $\varphi^*(x)$ is the box function in the interval $[0, 1]$, and for the linear scaling function, $\varphi^*(x)$ is the hat function. Example for α_n when $\varphi^*(x)$ is chosen as a hat function is given in Table 1, and the corresponding scaling function is called the linear spline function. The wavelet coefficients d_n and the decomposition coefficient b_n for linear spline function are shown in Tables 2 and 3, respectively. Scaling and wavelet functions obtained from Haar and hat candidate function using Eqs. (13) and (14) are shown in Fig. 1.

The wavelet transformation is defined to transform functions in different scales

$$w_j : V_{j+1} \rightarrow V_j \oplus W_j, \tag{19}$$

Table 1
Orthogonal expansion coefficients for hat function ($\alpha_n = \alpha_{-n}$)

n	α_n
0	1.29167549215928E + 00
1	-1.74663234444464E - 01
2	3.52101152592182E - 02
3	-7.87442512950393E - 03

Table 2
Wavelet coefficients, d_n for linear spline function ($d_n = d_{-n}$)

n	d_n
0	8.17646057010934E - 01
1	3.97297088134191E - 01
2	-6.91009867416467E - 02
3	-5.19453480818384E - 02
4	1.69710478938706E - 02
5	9.99059544418377E - 03
6	-3.88326225090555E - 03
7	-2.20195123839720E - 03
8	9.23371005487156E - 04
9	5.11636022693058E - 04
10	-2.24296326726262E - 04

Table 3
Decomposition coefficient $b_n = b_{-n-2}$

n	b_n
-1	0.817646595961945
0	-0.397296919701700
1	-0.069101397548309
2	0.051944587049999
3	0.016972531859965
4	-0.009987734381633
5	-0.003888792672210
6	0.002191236880415
7	0.000944025366123
8	-0.000473612955027
9	-0.000315829481785
10	0.000036249000464

where w_j is an orthogonal operator which maps the basis $\{\varphi_{j+1,k}\}$ onto $\{\varphi_{j,k}, \psi_{j,k}\}$. We denote the L_2 -projection onto V_j and W_j by operators \mathbf{P}_j and \mathbf{Q}_j such that

$$\begin{aligned}
 \mathbf{P}_j &: V_{j+1} \rightarrow V_j, \\
 \mathbf{Q}_j &: V_{j+1} \rightarrow W_j.
 \end{aligned}
 \tag{20}$$

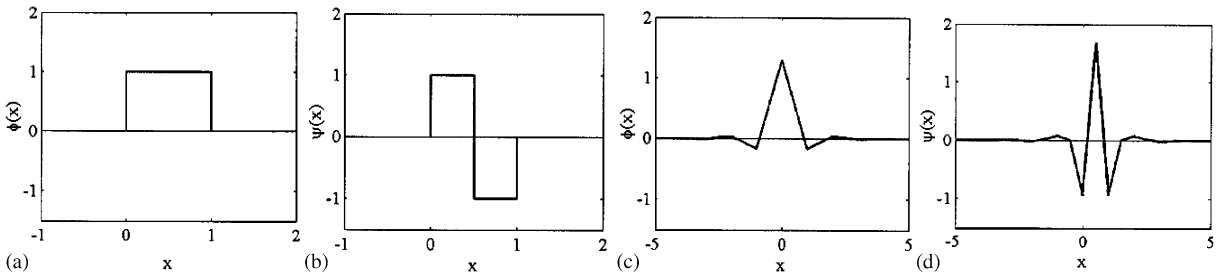


Fig. 1. (a) Haar scaling function; (b) corresponding wavelet; (c) linear orthogonal scaling function; (d) corresponding wavelet.

These wavelet and scaling functions in different scales are used as the hierarchical basis for wavelet-based multi-scale homogenization which are discussed in the next section. In case of using Haar basis, the discrete form of operators P_j and Q_j are given below:

$$P_j = \frac{1}{\sqrt{2}} \begin{bmatrix} 1 & 1 & 0 & 0 & \cdots & 0 & 0 \\ 0 & 0 & 1 & 1 & \cdots & 0 & 0 \\ \vdots & \vdots & \vdots & \vdots & \cdots & \vdots & \vdots \\ 0 & 0 & 0 & 0 & \cdots & 1 & 1 \end{bmatrix}_{2^{j-1} \times 2^j}, \tag{21}$$

$$Q_j = \frac{1}{\sqrt{2}} \begin{bmatrix} 1 & -1 & 0 & 0 & \cdots & 0 & 0 \\ 0 & 0 & 1 & -1 & \cdots & 0 & 0 \\ \vdots & \vdots & \vdots & \vdots & \cdots & \vdots & \vdots \\ 0 & 0 & 0 & 0 & \cdots & 1 & -1 \end{bmatrix}_{2^{j-1} \times 2^j} \tag{22}$$

As for scaling and wavelet functions constructed by the candidate hat function, the discrete form of operators P_j and Q_j are

$$P_j = \begin{bmatrix} d_{j-2k} & 0 & 0 & 0 & 0 & \cdots & 0 & 0 & 0 \\ d_{j-2(k+1)} & d_{j+1-2(k+1)} & d_{j+2-2(k+1)} & 0 & 0 & \cdots & 0 & 0 & 0 \\ d_{j-2(k+2)} & d_{j+1-2(k+2)} & d_{j+2-2(k+2)} & d_{j+3-2(k+2)} & d_{j+4-2(k+2)} & \cdots & 0 & 0 & 0 \\ \vdots & \vdots & \vdots & \vdots & \vdots & \vdots & \vdots & \vdots & \vdots \\ 0 & 0 & 0 & 0 & 0 & \cdots & d_{j+m-2-2(k+n-1)} & d_{j+m-1-2(k+n-1)} & d_{j+m-2(k+n-1)} \\ 0 & 0 & 0 & 0 & 0 & \cdots & 0 & 0 & d_{j+m-2(k+n)} \end{bmatrix}, \tag{23}$$

$$\mathbf{Q}_j = \begin{bmatrix} b_{j-2k} & 0 & 0 & 0 & 0 & \cdots & 0 & 0 & 0 \\ b_{j-2(k+1)} & b_{j+1-2(k+1)} & b_{j+2-2(k+1)} & 0 & 0 & \cdots & 0 & 0 & 0 \\ b_{j-2(k+2)} & b_{j+1-2(k+2)} & b_{j+2-2(k+2)} & b_{j+3-2(k+2)} & b_{j+4-2(k+2)} & \cdots & 0 & 0 & 0 \\ \vdots & \vdots & \vdots & \vdots & \vdots & \vdots & \vdots & \vdots & \vdots \\ 0 & 0 & 0 & 0 & 0 & \cdots & b_{j+m-2-2(k+n-1)} & b_{j+m-1-2(k+n-1)} & b_{j+m-2(k+n-1)} \\ 0 & 0 & 0 & 0 & 0 & \cdots & 0 & 0 & b_{j+m-2(k+n)} \end{bmatrix}, \tag{24}$$

where k , n , and m are related to the non-zero coefficients of the sequence d_i and b_i . The coefficients d_i and b_i as defined in Eq. (18) are tabulated in Tables 2 and 3.

3. Wavelet-based homogenization using projection method

The multiresolution strategy for the homogenization of linear problems using wavelets was first addressed by Brewster and Beylkin [4]. Let the discrete form of the boundary value problem be expressed by

$$\mathbf{L}U = \mathbf{F} \tag{25}$$

augmented by boundary conditions, where \mathbf{L} is a bounded linear operator. Let the above mentioned discrete equation be formed in the space V_{j+1} , i.e.

$$\mathbf{L}_{j+1}U_{j+1} = \mathbf{F}_{j+1}, \tag{26}$$

where operator \mathbf{L}_{j+1} acts on the space V_{j+1} and is constructed by the basis functions spanning V_{j+1} . In Eq. (26), subscript denotes the level of the resolution. Consider the decomposition of the scaling function spaces

$$V_{j+1} = V_j \oplus W_j. \tag{27}$$

Using the discrete projecting operators \mathbf{P}_j and \mathbf{Q}_j defined in Eq. (20), fine and coarse scale components of U_{j+1} can be extracted as follows:

$$\mathbf{w}_j = \begin{bmatrix} \mathbf{Q}_j \\ \mathbf{P}_j \end{bmatrix}, \tag{28}$$

$$\mathbf{w}_j U_{j+1} = \mathbf{w}_j U_{j+2}^l = \begin{bmatrix} U_{j+1}^h \\ U_{j+1}^l \end{bmatrix}, \tag{29}$$

$$U_{j+1}^l = \mathbf{P}_j U_{j+1}, \quad U_{j+1}^l \in V_j, \quad U_{j+1} \in V_{j+1}, \tag{30}$$

$$U_{j+1}^h = \mathbf{Q}_j U_{j+1}, \quad U_{j+1}^h \in W_j, \tag{31}$$

where the function U_{j+1} is split into a low scale component U_{j+1}^l as a projection onto V_j , and high-scale component U_{j+1}^h as a projection onto W_j , \mathbf{w}_j is the wavelet transformation operator, and

the superscripts h and l denote the high- and low-scale components, respectively. By performing the transformation of Eq. (28), we have

$$(\mathbf{w}_j \mathbf{L}_{j+1} \mathbf{w}_j^T)(\mathbf{w}_j \mathbf{U}_{j+1}) = \begin{bmatrix} \mathbf{L}_{11} & \mathbf{L}_{12} \\ \mathbf{L}_{21} & \mathbf{L}_{22} \end{bmatrix}_{j+1} \begin{bmatrix} \mathbf{U}_{j+1}^h \\ \mathbf{U}_{j+1}^l \end{bmatrix} = \mathbf{w}_j \mathbf{F}_{j+1} = \begin{bmatrix} \mathbf{F}_{j+1}^h \\ \mathbf{F}_{j+1}^l \end{bmatrix}, \tag{32}$$

where

$$\begin{bmatrix} \mathbf{F}_{j+1}^h \\ \mathbf{F}_{j+1}^l \end{bmatrix} = \begin{bmatrix} \mathbf{Q}_j \mathbf{F}_{j+1} \\ \mathbf{P}_j \mathbf{F}_{j+1} \end{bmatrix} \tag{33}$$

in which \mathbf{F}_{j+1}^h and \mathbf{F}_{j+1}^l denote the high- and low-scale components of \mathbf{F}_{j+1} . Note that \mathbf{w}_j is an orthogonal transformation, i.e., $\mathbf{w}_j^T \mathbf{w}_j = \mathbf{I}$.

The low-scale component \mathbf{U}_{j+1}^l is obtained by the Schur complement of \mathbf{L}_{11} in Eq. (32) to yield

$$(\mathbf{L}_{22} - \mathbf{L}_{21} \mathbf{L}_{11}^{-1} \mathbf{L}_{12})_{j+1} \mathbf{U}_{j+1}^l = \mathbf{F}_{j+1}^l - \mathbf{L}_{21} \mathbf{L}_{11}^{-1} \mathbf{F}_{j+1}^h \tag{34}$$

in which the Schur complement is defined as

$$\bar{\mathbf{L}}_{j+1} = (\mathbf{L}_{22} - \mathbf{L}_{21} \mathbf{L}_{11}^{-1} \mathbf{L}_{12})_{j+1}, \tag{35}$$

where $\bar{\mathbf{L}}_{j+1}$ is the coarse scale operator, and is also called the one-step reduction of the operator \mathbf{L}_{j+1} . Note that the solution \mathbf{U}_{j+1}^l of the reduced equation is exactly $\mathbf{P}_j \mathbf{U}_{j+1}$. The Schur complement in Eq. (34) acts on the coarser subspace $V_j \subset V_{j+1}$. In the case when only the coarse-scale component is desired, it is sufficient to solve Eq. (34).

A multi-scale homogenization is performed by first solving the solution at the finest scale. Upon obtaining the solution of one scale, the low- and high-scale components of the next coarser level can be calculated by wavelet transformation in Eqs. (30) and (31). These high- and low-scale components are due to the projection of V_{j+1} onto W_j and V_j , respectively. We may apply this projection recursively to produce the solution on V_{j-n} for any coarser level. Thus multi-scale homogenization procedure can be carried out by generating a sequence of homogenized equations. Conversely, localization is a reverse process of homogenization, in which the fine scale component at each scale can be recovered by backward substitution of coarse scale solution, i.e.

$$(\mathbf{L}_{11})_{j+1} \mathbf{U}_{j+1}^h = \mathbf{F}_{j+1}^h - (\mathbf{L}_{12})_{j+1} \mathbf{U}_{j+1}^l \tag{36}$$

and the low-scale solution of next finer scale can be obtained by

$$\mathbf{U}_{j+2}^l = \mathbf{w}_j^{-1} \begin{bmatrix} \mathbf{U}_{j+1}^h \\ \mathbf{U}_{j+1}^l \end{bmatrix} = \mathbf{w}_j^{-1} \begin{bmatrix} \mathbf{U}_{j+1}^h \\ \mathbf{U}_j \end{bmatrix}. \tag{37}$$

In this localization operation, Eq. (36) is referred to as reconstruction of the high-scale component using the corresponding low-scale component, and Eq. (37) represents the recovery of the low-scale component of the next finer level. By repeating these two operations, solution of any finer scale can be hierarchically reconstructed. The procedures of the homogenization and localization are illustrated

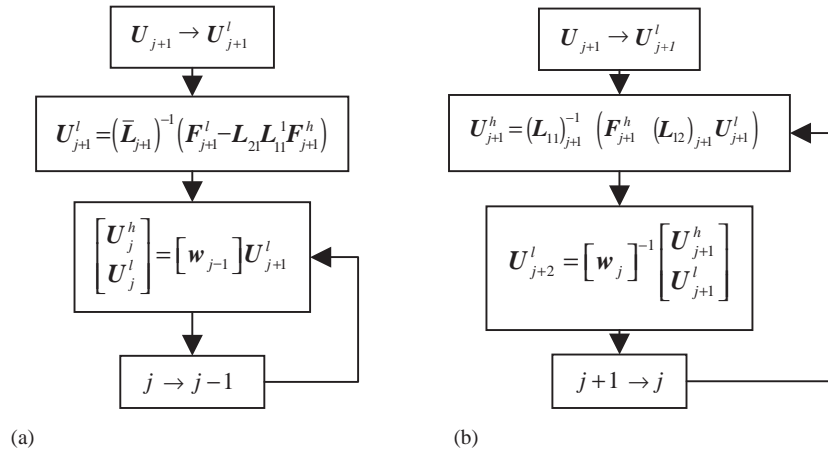


Fig. 2. (a) Homogenization and (b) localization processes.

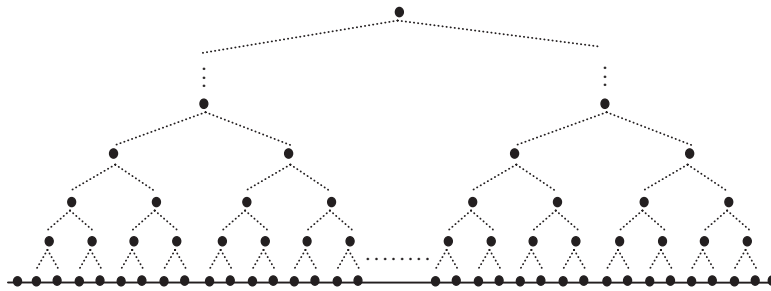


Fig. 3. Data compactness through the reduction process of wavelet-based homogenization.

and compared in Fig. 2. These methods of homogenization and localization can be easily extended to higher dimensions.

4. Data compactness and mirror image technique

As shown in Fig. 3, at the coarser levels we have less data points with respect to the finer levels. This is due to the fact that information at each coarse scale node is provided by some adjacent nodes at finer scale. As a consequence, at the coarse levels data information is only available at the nodes toward the center of the domain. If no information is provided for the points outside of the domain, the zero coefficients associated with the representative data points outside the domain of response will pollute the whole solution after few steps of homogenization process. The proposed remedy for this problem is a mirror image technique by extending the physical domain with solution data to a fictitious domain with anti-symmetric data as shown in Fig. 4. In this case the average of solution at boundaries remains unchanged. Hence, this process does not generate any projection onto the wavelet spaces since the wavelet projection filters out the deviation from the average.

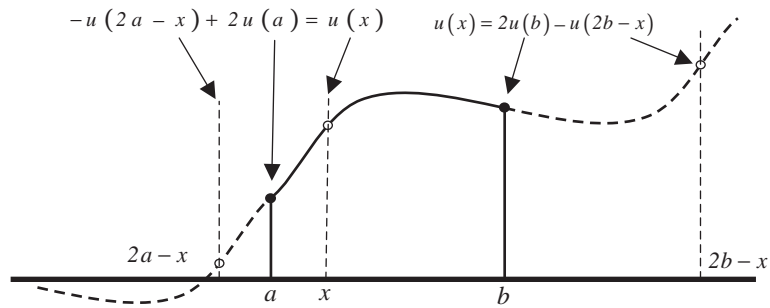


Fig. 4. Mirror image data construction in the fictitious domain (a and b : boundaries of real domain).

5. Numerical examples

In this section, the following 1-D elasticity model problem depicted in Fig. 5 with highly oscillatory Young’s modulus as shown in Fig. 6 is considered to examine the effectiveness of the proposed

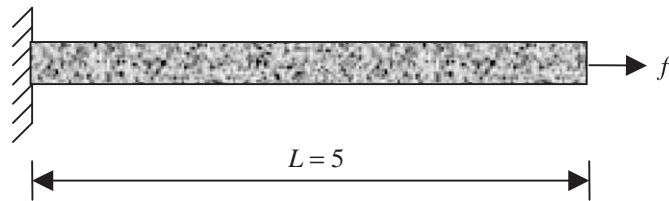


Fig. 5. Highly inhomogeneous bar.

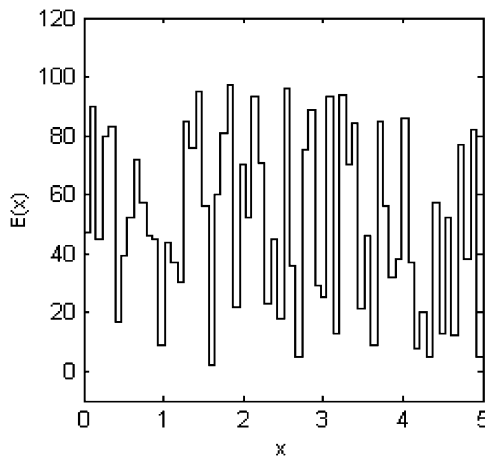


Fig. 6. Young’s modulus distribution.

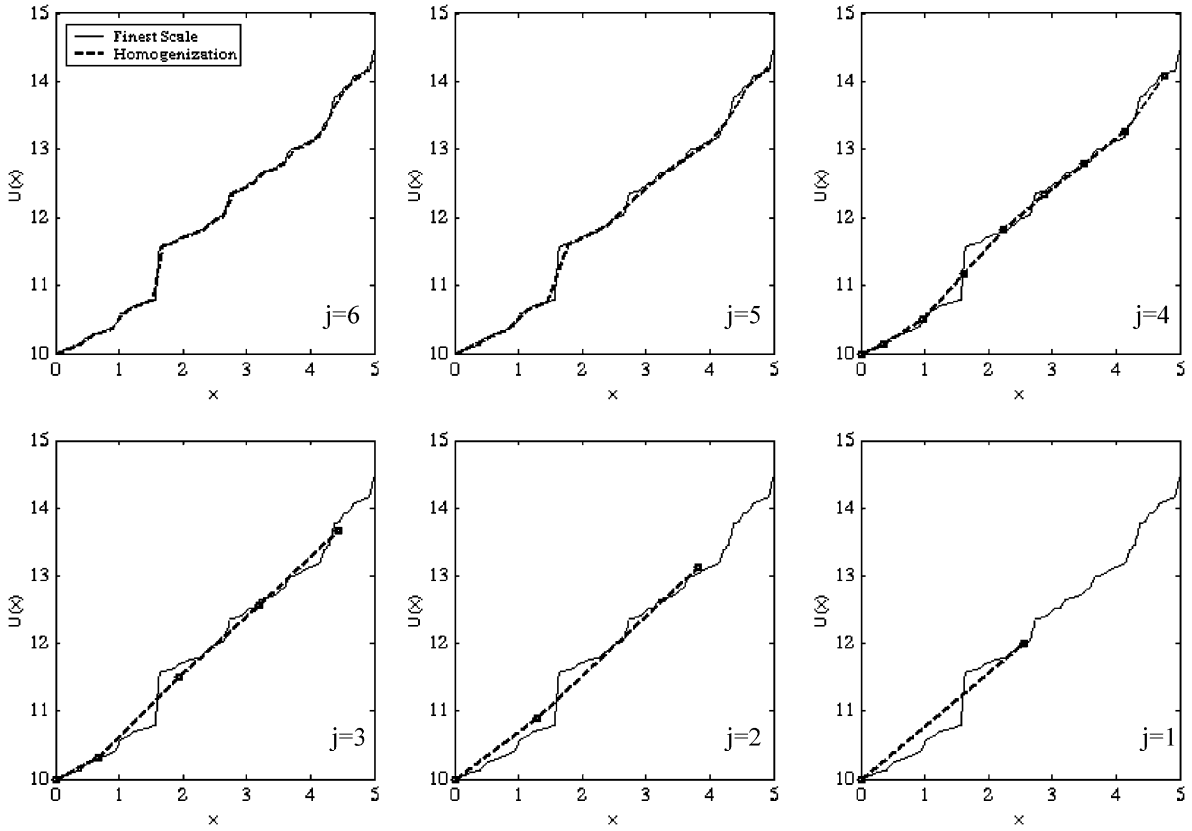


Fig. 7. Wavelet-based homogenization over multiple scales using Haar basis (j : level of resolution, $u(0) = 10$, $u'(5) = 4$).

wavelet-based projection method

$$\frac{d}{dx} \left(E(x) \frac{du(x)}{dx} \right) = 0, \quad x \in (0, 5). \tag{38}$$

We contemplate two different boundary conditions:

$$\begin{cases} u(0) = 10, \\ u'(5) = 4, \end{cases} \tag{39}$$

$$\begin{cases} u(0) = 10, \\ u(5) = 20. \end{cases} \tag{40}$$

To illustrate key features of the proposed method, we consider the following three cases of wavelet and scaling functions in multi-scale homogenization:

- (1) Orthogonal wavelet and scaling functions of Haar system.
- (2) Orthogonal wavelet and scaling functions generated by the hat function without mirror image technique.

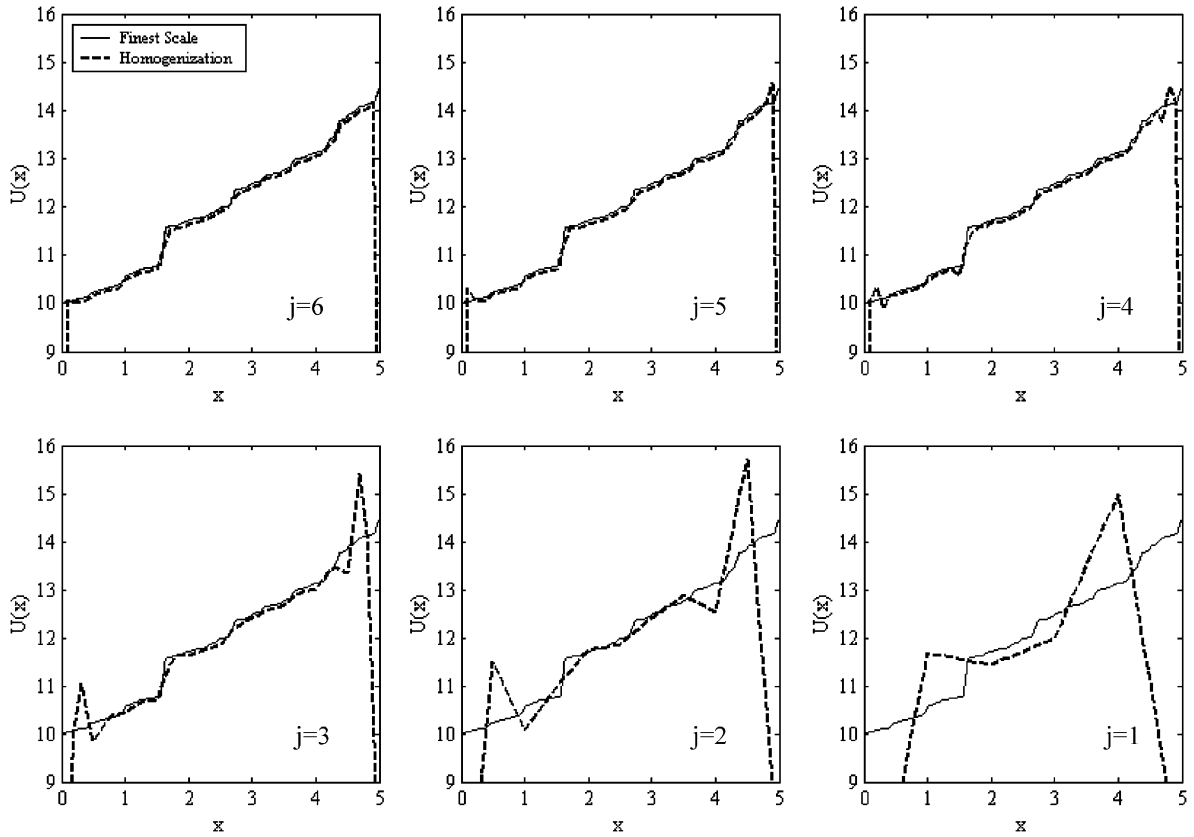


Fig. 8. Wavelet-based homogenization using linear orthogonal scaling function and wavelet without using mirror image technique (j : level of resolution, $u(0) = 10$, $u'(5) = 4$).

(3) Orthogonal wavelet and scaling functions used in case (2) with employment of mirror image technique.

In the proposed wavelet projection method, the fine scale solution can be obtained by any numerical methods. A finite element method has been used herein to obtain the fine scale solution. To capture the fine scale details of the solution, the finest grid associated with the finest scale of the solution is considered to have the nodal distance of $5(\frac{1}{2})^6$ ($j = 6$).

In the first case, Haar system is employed, and boundary conditions of Eq. (39) are imposed. Similar to what has been proposed in [5], while the interpolation of essential boundary condition can be correctly imposed in the homogenization process, the natural boundary condition cannot be properly interpolated using Haar basis as shown in Fig. 7.

In the second case, we use linear orthogonal scaling and wavelet functions as shown in Fig. 1(c) and (d) without using the mirror image technique. Boundary conditions of Eq. (39) are introduced. As shown in Fig. 8, errors accumulate near the boundaries. Further, the solution renders oscillation near the boundaries at each scale, and the oscillation increases as the homogenization proceeds to

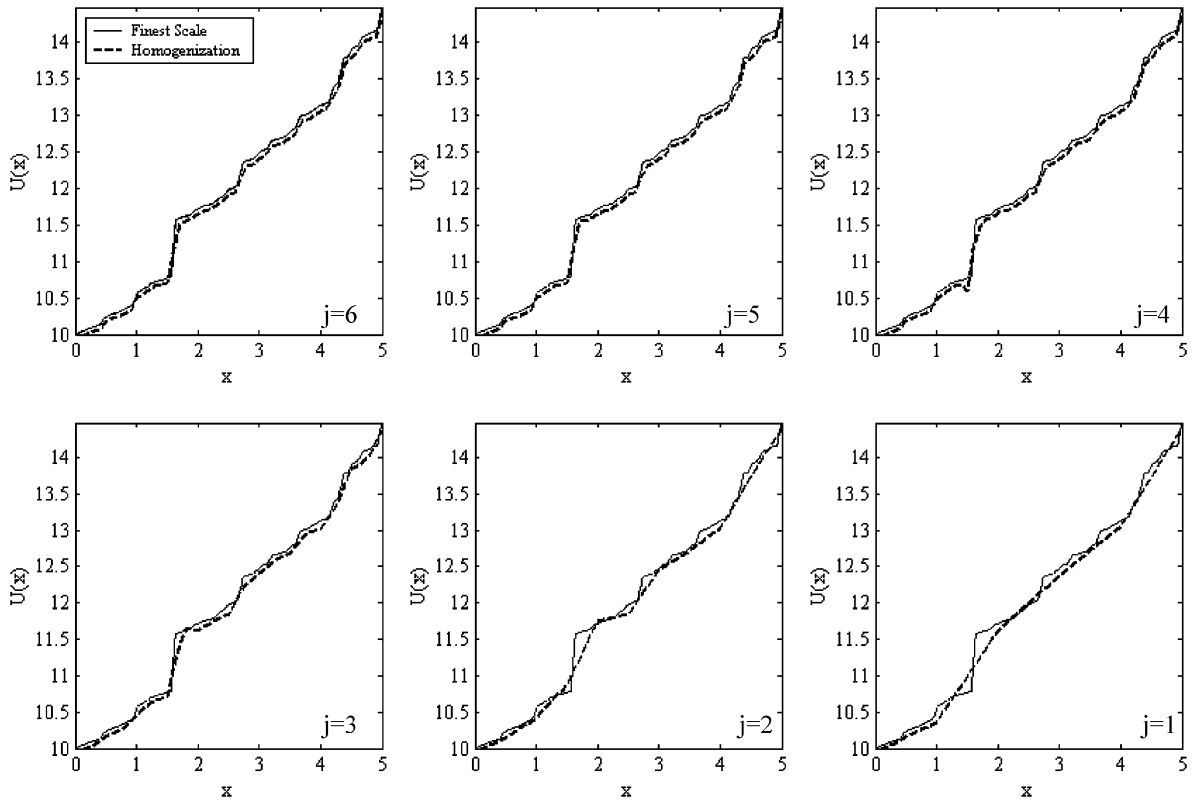


Fig. 9. Wavelet-based homogenization using linear orthogonal scaling function and wavelet, and mirror image technique (j : level of resolution, $u(0) = 10$, $u'(5) = 4$).

the coarser scales. This is due to the absence of data outside of the problem domain. This oscillation in the homogenized solution is corrected by using the mirror image technique in the third case as shown in Fig. 9. Since the wavelet projection filters out the deviation from the average, the mirror image process does not generate any projection onto to wavelet spaces and thus maintains the accuracy of the boundary conditions. Note that at each scale the high-scale components (high oscillations) are filtered out from the solution. After a few steps of the homogenization process, sufficiently coarse component of the solution can be captured. The same method is also applicable to the case with boundary conditions in Eq. (40) as demonstrated in Fig. 10. Unlike the asymptotic method, this method provides all the intermediate scales through which homogenization is being done. In addition, the method is applicable to the problems even if the material property is not periodic (no unit cell exists).

6. Conclusion

The wavelet-based multi-scale projection method has been introduced to provide a systematic approach for multi-scale homogenization of highly heterogeneous materials. By means of the wavelet

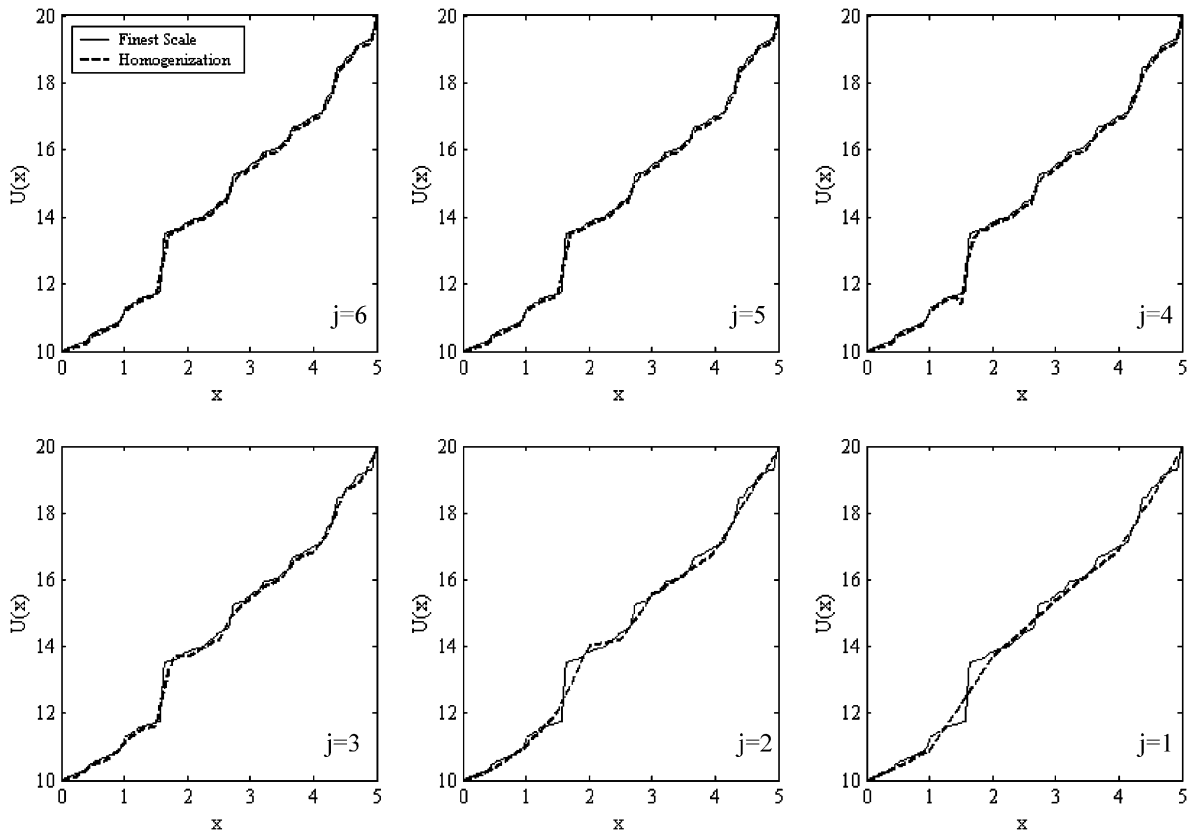


Fig. 10. Wavelet-based homogenization using linear orthogonal scaling function and wavelet, and mirror image technique (j : level of resolution, $u(0) = 10$, $u(5) = 20$).

transformation in which wavelets and corresponding scaling functions are used as the bases, the obtained solution is projected onto the scaling and wavelet spaces resulting in the decomposition of high- and low-scale components of the solution at any scale. Repetition of such a projection results in multi-scale homogenization of the fine scale solution. In the localization process, the coarse and fine scale component of the solution at any scale can be used to reconstruct the coarse scale solution of the finer level.

In this study, the Haar system and the linear orthogonal scaling and wavelet functions based on the hat function have been constructed as the basis functions in wavelet transformation. By means of projection onto the wavelet spaces, homogenization of the solution of elasticity model problem with oscillatory Young's modulus has been carried out. In this approach, the fine scale solution can be obtained by any kind of numerical methods. In this work, a finite element method has been used in obtaining the fine scale solution. In order to correctly interpolate information at the boundaries during the process of homogenization, wavelet-based projection onto the linear orthogonal wavelet and scaling function spaces has been introduced. The transformation matrix corresponding to linear orthogonal wavelet and scaling functions constructed by the hat function as the mother

scaling function has also been derived for multi-scale homogenization. Moreover, the mirror image technique has been employed to preserve the accurate representation of boundary conditions and to avoid numerical oscillation near the boundaries. Since the wavelet projection filters out the deviation from the average, the mirror image process does not generate any projection onto to wavelet spaces and thus maintains the accuracy of the boundary conditions.

Numerical examples have been presented to demonstrate the effectiveness of the proposed methods. The comparison of the multi-scale homogenization using Haar system and linear orthogonal scaling function and wavelet are also elucidated.

Acknowledgements

The support of this work by NSF under Grant CMS 0084589 to University of California, Los Angeles is greatly acknowledged.

References

- [1] A. Bensoussan, J.L. Lions, G. Papanicolau, *Asymptotic Analysis for Periodic Structures*, North Holland, Amsterdam, 1978.
- [2] J.T. Oden, K. Vemaganti, N. Moes, Hierarchical modeling of heterogeneous solids, *Comput. Methods Appl. Mech. Eng.* 172 (1999) 3–25.
- [3] J. Fish, V. Belsky, Multi-grid method for periodic heterogeneous media, part 1: convergence studies for one-dimensional case, *Comput. Methods Appl. Mech. Eng.* 126 (1995) 1–16.
- [4] M. Brewster, G. Beylkin, A multiresolution strategy for numerical homogenization, *Appl. Comput. Harmon. Anal.* 2 (1995) 327–349.
- [5] M. Dorobantu, B. Engquist, Wavelet-based numerical homogenization, *SIAM J. Numer. Anal.* 35 (2) (1998) 540–559.
- [6] N.A. Coult, A multiresolution strategy for homogenization of partial differential equations, Ph.D. Thesis, Department of Applied Mathematics, University of Colorado, 1997.
- [7] S. Knapek, Matrix-dependant multi-grid homogenization for diffusion problems, preprint, 1996.
- [8] R. Glowinski, W. Lawton, M. Ravachol, E. Tenenbaum, Wavelet solution of linear and nonlinear elliptic, parabolic, and hyperbolic problems in one space dimension, *Proceedings of the 9th International Conference on Numerical Methods in Applied Sciences and Engineering*, SIAM, Philadelphia, 1990.
- [9] I. Daubechies, *Ten Lectures on Wavelets*, CBMS-NSF Series in Applied Mathematics, SIAM, Philadelphia, 1992.
- [10] C.K. Chui, *An Introduction to Wavelets*, Academic Press, New York, 1992.
- [11] A. Boggess, F.J. Narcowich, *A First Course in Wavelets with Fourier Analysis*, Prentice-Hall, Englewood Cliffs, NJ, 2001.